Advanced Steel Construction – Vol. 16 No. 3 (2020) 191–205
DOI:10.18057/IJASC.2020.16.3.1

AN IMPROVED EXPLICIT-IMPLICIT PRECISE INTEGRATION METHOD FOR NONLINEAR DYNAMIC ANALYSIS OF STRUCTURES

Zhi-Xia Ding [1], Zuo-Lei Du [1], Wei Su [2, *] and Yao-Peng Liu [1, 3]

[1] *Department of Civil and Environmental Engineering, The Hong Kong Polytechnic University, Hung Hom, Kowloon, Hong Kong, China*
[2] *School of Aeronautics and Astronautics, Sun Yat-sen University, Guangzhou, 510275, China*
[3] *Nida Technology Co. Ltd., Hong Kong Science Park, Shatin, N.T., Hong Kong, China*
** (Corresponding author: E-mail: suwei@mail.sysu.edu.cn)*

ABSTRACT

In this paper, an improved explicit-implicit precise integration method (EIPIM) is proposed for nonlinear dynamic analysis of structures based on the refined precise integration method (RPIM). The RPIM may face a numerical instability problem when using large time steps while the proposed EIPIM uses an explicit predictor–implicit corrector scheme to provide more stable and accurate results and allow for large time steps. When using EIPIM, the unknown displacements at the starting point are predicted by an explicit function, and the trial displacements at the second step are corrected by the implicit Lagrange interpolation method. In terms of numerical stability and precision, eight explicit formulas have been evaluated to develop a better predictor for EIPIM, i.e., two third-order, four fourth-order and two fifth-order functions. Four examples involving both linear and nonlinear problems illustrate the high stability and numerical efficiency of the proposed method. It is found that the explicit predictors EIPIM_O31 and EIPIM_O41 show good performance and are recommended for nonlinear dynamic analysis.

ARTICLE HISTORY

Received: 11 May 2019
Revised: 19 November 2019
Accepted: 15 December 2019

KEYWORDS

Precise integration method;
Nonlinear dynamic analysis;
Explicit predictor–implicit corrector scheme;
Stability and accuracy

1. Introduction

Wind-induced response [1] and wave-induced response [2] are the two important applications of dynamic analysis in the design process of offshore steel structures. The precise integration method (PIM) with high accuracy and explicit recursion was firstly proposed by Zhong and Williams [3-4] for structural dynamic analysis. In the past decsades, many researchers made significant contributions on the development and improvement of PIM. Nowadays, it has been applied to many fields, including optimal control, heat conduction, wave propagation, partial differential equation, etc. [5]. The concept of PIM is to convert the second-order ordinary differential equation (ODE) to a first-order ODE by introducing a vector, through which more accurate results can be obtained with high numerical stability. Nevertheless, the size of matrices is doubled when using PIM, leading to increased computational efforts. Many efforts have been made to reduce computational efforts [6-8] and handle nonlinear inhomogeneous parts [9-11]. However, very few studies focused on incorporating PIM into the nonlinear structural dynamic analysis. Zhang et al. [12] incorporated PIM into dynamic elastic-plastic hardening and softening problems in which only a motion equation with constant stiffness matrices is involved. The authors of this paper proposed the refined precise integration method (RPIM) [13], introducing a new vector representing velocity that is an improvement over Zhong [3-4, 14] and Gao [15]. In this method, the operation on doubled matrices is simplified to the operation on 2×2 matrices. The stiffness matrix is treated as an unknown variable to adapt RPIM into nonlinear structural problems. However, similar to other explicit and implicit methods [16], the stability problem may also occur when a large time increment is adopted even though RPIM is unconditionally stable with a spectral radius of less than 1.

Both implicit and explicit methods are employed in commercial or uncommercial packages for structural analysis, for example, ABAQUS [17] and OpenSees [18]. The explicit procedures, such as the central difference method (CDM), are conditionally stable and demand smaller time increments to achieve accurate results. Implicit procedures, such as the Newmark method [19], trapezoidal rule [20], and Wilson θ-method [21], are unconditionally stable in the linear analysis but can become unstable in the nonlinear analysis [16]. Though explicit methods avoid the procedure of iteration, having been explored by many researchers[22-23], truncation error during the procedure will be accumulated and lead to inaccurate results or difficulty in convergence. For implicit methods, the error will be eliminated through several steps of iteration, and the accuracy of results is guaranteed within pre-defined tolerance. Therefore, the implicit methods can employ larger time increments. The composite implicit time integration method is a procedure with two sub-steps per time step and the two times computational effort for a certain time step size is compensated unconditionally by the achieved stability. Bathe [16, 24] extended the trapezoidal rule by combing with the three-point Euler backward method in the second sub-step, and it is verified to be unconditional stability. This method was also proved to be applicable for large time step sizes in both linear and nonlinear structural analysis of very flexible and stiff problems [25-26]. Zhang et al. [27] studied the accuracy of a generalized composite implicit method combining the Newmark method and three-point backward Euler method, and then an accuracy analysis framework was recommended for composite schemes. Kim and Choi [28] improved an implicit composite time integration algorithm with the weighted residual method for linear analysis, and the weighting parameters are optimized with a single degree of freedom (DOF) problem. In these studies, the results with second order accuracy as well as unconditional stability was achieved.

To incorporate the excellent stability of implicit methods into the explicit method, many researchers developed the adaptive explicit method, in which an adaptive time stepping procedure is adopted to control time discretization error in each step [29]. One of the most popular adaptive strategies is the local error estimator incorporated in each step. The adaptive Rung-Kutta method [30-31] provides an estimation of the local truncation error of a single Rung-Kutta step; thus, the error can be controlled within a limit by changing to a smaller step, which can be automatically selected. The automatic time step control strategy by Hulbert and Jang [32], based on the derived local error estimator was demonstrated with reliable step size behavior. Deokar et al. [33] proposed an independent posteriori error estimator based on the generalized single step single solve (GSSSS) framework and adaptive time steps saved much computational effort. Wang and Zhong [34] employed a priori error analysis in the proposed time finite element method for structural dynamics. Mayr et al. [35] developed an adaptive time stepping scheme for fluid-structure interaction (FSI) problems with a posteriori error estimation by comparing two different schemes. Meanwhile, other adaptive strategies on numerical time integration for dynamic structural analysis, such as the algorithm of Bergan and Mollestad based on current characteristic frequency, and the method of Lages et al. based on the geometric indicator of displacements history curvature, have been studied by researchers [36]. Although the adaptive strategies have advantages in terms of accuracy and efficiency, they are difficult to incorporate into RPIM because their coefficients have to be recalculated for a different time increment. Nevertheless, the idea of estimation in each step could be combined with RPIM to improve stability [37].

Inspired by composite implicit methods and adaptive time stepping procedures, an explicit-implicit precise integration method (EIPIM) is proposed in this paper. We propose RPIM to deal with nonlinear dynamic problems based on PIM by Zhong [3] and an additional theorem of Duhamel integration by Tan [38]. The unconditional spectral stability and high accuracy of RPIM have been verified. To possess the advantages of both explicit and implicit methods, explicit functions are employed in EIPIM to estimate

displacements for the next step while the implicit Lagrange interpolation method is adopted in the recursion formula. Eight estimation functions with three different orders of accuracy are proposed and evaluated in this paper, both theoretically and practically. We employed four cases involving beam element, truss element, and shell element to test and verify the stability and efficiency of EIPIMs with different estimation functions for both linear and nonlinear dynamic analysis of structures.

2. Conventional central difference method

In dynamic structural problems, the equation of motion is defined as

$$\mathbf{M}\ddot{\boldsymbol{x}} + \mathbf{C}\dot{\boldsymbol{x}} + \mathbf{K}\boldsymbol{x} = \mathbf{f}(\boldsymbol{x}, \mathrm{t}) \tag{1}$$

in which, M, C, and K are the mass, damping, and stiffness matrices of the structural system respectively; $\mathbf{f}(\boldsymbol{x}, \mathrm{t})$ is the external force vector related to time and displacements. $\boldsymbol{x}$, $\dot{\boldsymbol{x}}$, and $\ddot{\boldsymbol{x}}$ are the displacement, velocity, and acceleration vectors of each DOF.

The velocity and acceleration are written as

$$\dot{\boldsymbol{x}}_{t+\Delta t/2} = (\boldsymbol{x}_{t+\Delta t} - \boldsymbol{x}_t)/\Delta t \tag{2}$$

$$\ddot{\boldsymbol{x}}_t = \left(\dot{\boldsymbol{x}}_{t+\Delta t/2} - \dot{\boldsymbol{x}}_{t-\Delta t/2}\right)/\Delta t \tag{3}$$

where $\boldsymbol{x}$ is a DOF (e.g., displacement or rotation), the subscript t refers to the current time step and Δt refers to the time increment in the dynamic analysis.

The CDM is conditionally stable with the stability limit given in terms of the system or the elements as

$$\Delta t \le \frac{2}{\omega_{\max}} \tag{4}$$

$$\Delta t \le \frac{2}{\omega_{\max}^{element}} \tag{5}$$

in which $\omega_{\max}$ is the highest eigenvalue of the system and $\omega_{\max}^{element}$ is the maximum eigenvalue of elements.

The estimation for Δt is only approximate and in most cases is not a conservative estimation [17]. In the nonlinear analysis, the stable time limit is going to change with the highest frequency of model; and thus, the time increment has to be estimated at every step. Otherwise, a small enough time increment should be used to ensure stable solutions. An approximation to the stable time limit can also be written as the smallest transit time of a dilatational wave across any of the elements in the mesh, which clearly demonstrates the relationship between stable time limit and element size.

3. RPIM for dynamic structural problems

To deal with nonlinear dynamic analysis, the authors proposed the RPIM based on the traditional PIM [3] and the additional theorem of Duhamel integration derived by Tan [39]. A new vector p, representing velocity is employed, and the matrix for coefficients calculation is converted to a 2×2 matrix, significantly simplifying the computation and saving storage space.

3.1. Refined precise integration method (RPIM)

The authors proposed RPIM to deal with nonlinear dynamic problems in which the stiffness matrix K varies with time in elastic-plastic range. The third item, $\mathbf{K}\boldsymbol{x}$ in equation of motion Eq.(1) is considered as an unknown variable, and a new vector $\mathbf{F}(\boldsymbol{x}, t)$ combining the external force vector $\mathbf{f}(\boldsymbol{x}, t)$ and internal force Kx is formed. Then, the equation of motion can be rewritten as

$$\mathbf{M}\ddot{\boldsymbol{x}} + \mathbf{C}\dot{\boldsymbol{x}} = \mathbf{f}(\boldsymbol{x}, t) - \mathbf{K}\boldsymbol{x} = \mathbf{F}(\boldsymbol{x}, t) \tag{6}$$

A new vector p, representing the velocity, is introduced as

$$\boldsymbol{p} = \dot{\boldsymbol{x}} \tag{7}$$

Writing Eq.(6) and Eq.(7) in matrix form,

$$\boldsymbol{u} = \begin{bmatrix} \boldsymbol{x} \\ \dot{\boldsymbol{x}} \end{bmatrix}, \qquad \boldsymbol{u} = \mathbf{H}\boldsymbol{u} + \mathbf{F} \tag{8}$$

in which

$$\mathbf{H} = \begin{bmatrix} \mathbf{0} & \boldsymbol{I} \\ \mathbf{0} & -\mathbf{M}^{-1}\mathbf{C} \end{bmatrix} \tag{9}$$

$$\mathbf{F} = \begin{bmatrix} \mathbf{0} \\ \mathbf{F}(\boldsymbol{x}, t) \end{bmatrix} = \begin{bmatrix} \mathbf{0} \\ \mathbf{M}^{-1}\mathbf{f}(\boldsymbol{x}, t) - \mathbf{M}^{-1}\mathbf{K}\boldsymbol{x} \end{bmatrix} \tag{10}$$

The absolute solution of Eq.(8) with Duhamel integral is given mathematically as Eq.(11).

$$\boldsymbol{u}(\mathrm{t}) = \exp(\mathbf{H}t)\,\boldsymbol{x}(0) + \int_0^t \exp\big(\mathbf{H}(t-\tau)\big)\,\mathbf{F}(x,\tau)d\tau \tag{11}$$

The total time is divided into a series of step time η for numerical integration, and such that the time points are given as,

$$t_0 = 0,\ t_1 = \eta,\ t_2 = 2\eta, \dots,\ t_k = k\eta,\ t_{k+1} = (k+1)\eta, \dots \tag{12}$$

The integration equation of Eq.(11) can be given as Eq.(13) with the mark uk representing u(k) and t_k representing $t(k)$.

$$\boldsymbol{u}_{k+1} = \boldsymbol{\Phi}\boldsymbol{u}_k + \int_0^{\eta} \exp\big(\mathbf{H}(t_k - \tau)\big)\,\mathbf{F}(\boldsymbol{x}_k, \tau)\,d\tau \tag{13}$$

In which the matrix exponent is defined as Eq.(14), and the additional theorem is proposed by Zhong [3] to give an accurate solution.

$$\boldsymbol{\Phi} = \exp(\mathbf{H}\eta) \tag{14}$$

For more easy integration, the formed 'external force' $\mathbf{F}(\boldsymbol{x}, t)$ is written in polynomial form as,

$$\mathbf{F}(\boldsymbol{x}_k, t_k + \tau) = \boldsymbol{f}_{0,k} + \tau\boldsymbol{f}_{1,k} + \cdots + \tau^m\boldsymbol{f}_{m,k} \quad \tau \in [0, \eta] \tag{15}$$

The recursion formula can then be derived as Eq.(16) by substituting Eq.(15) into the general solution in Eq.(13).

$$\boldsymbol{v}_{k+1} = \boldsymbol{\Phi}\boldsymbol{v}_k + \eta\boldsymbol{\Phi}_0\boldsymbol{f}_{0,k} + \cdots + \eta^{m+1}\boldsymbol{\Phi}_m\boldsymbol{f}_{m,k} \tag{16}$$

in which,

$$\boldsymbol{\Phi}_m = \frac{1}{\eta^{m+1}}\int_0^{\eta} \exp\big(\mathbf{H}(\eta - \tau)\big)\,\tau^m\,d\tau \tag{17}$$

The additional theorem of Duhamel integration by Tan [38] can then be employed to achieve precise coefficients $\boldsymbol{\Phi}_m$ with the combination of the exponential matrix by Zhong [3].

With the coefficient β in Rayleigh damping [40] ignored, the damping matrix C is only proportional to the mass matrix M and then the $\mathbf{H}$ matrix is simplified as a 2×2 matrix. Thus, the coefficient matrix $\boldsymbol{\Phi}$ becomes a matrix with two different constant coefficients described as $\boldsymbol{\Phi}'$, and only constant elements exist in coefficients $\boldsymbol{\Phi}_0$, $\boldsymbol{\Phi}_1$, $\boldsymbol{\Phi}_2$, and $\boldsymbol{\Phi}_3$, as well as the linear operation results $\bar{\boldsymbol{\Phi}}_0$, $\bar{\boldsymbol{\Phi}}_1$, $\bar{\boldsymbol{\Phi}}_2$, and $\bar{\boldsymbol{\Phi}}_3$.

$$\boldsymbol{\Phi}' = \begin{bmatrix} 1 & c_1 \\ 0 & c_2 \end{bmatrix} \tag{18}$$

$$\boldsymbol{\Phi}_0 = \begin{bmatrix} \Phi_{01} \\ \Phi_{02} \end{bmatrix}, \boldsymbol{\Phi}_1 = \begin{bmatrix} \Phi_{11} \\ \Phi_{12} \end{bmatrix}, \boldsymbol{\Phi}_2 = \begin{bmatrix} \Phi_{21} \\ \Phi_{22} \end{bmatrix}, \boldsymbol{\Phi}_3 = \begin{bmatrix} \Phi_{31} \\ \Phi_{32} \end{bmatrix} \tag{19}$$

$$\bar{\boldsymbol{\Phi}}_0 = \begin{bmatrix} \bar{\Phi}_{01} \\ \bar{\Phi}_{02} \end{bmatrix}, \bar{\boldsymbol{\Phi}}_1 = \begin{bmatrix} \bar{\Phi}_{11} \\ \bar{\Phi}_{12} \end{bmatrix}, \bar{\boldsymbol{\Phi}}_2 = \begin{bmatrix} \bar{\Phi}_{21} \\ \bar{\Phi}_{22} \end{bmatrix}, \bar{\boldsymbol{\Phi}}_3 = \begin{bmatrix} \bar{\Phi}_{31} \\ \bar{\Phi}_{32} \end{bmatrix}$$

Thus, the multiplication between matrices and vectors becomes simple multiplication between constant values and vectors, and a large amount of computation time and memory size are saved; this is applicable to both consistent and lumped mass matrix for structures.

3.2. Implicit method for inhomogeneous term

Explicit method is adopted with Lagrange interpolation in the RPIM; however, inaccuracy and instability may occur with large time increment due to the integration in Eq.(13) over the time domain [tk, tk+1]. To alleviate this problem, an implicit method with three Lagrange integration points is adopted in the EIPIM.

The Lagrange polynomials 'external force' $\mathbf{F}(\boldsymbol{x}, t)$ within the time period $[t_k, t_{k+1}]$ with integration points t_{k+1}, t_k, t_{k-1}, t_{k-2} derived given as,

$$\begin{aligned} &\tilde{\mathbf{F}}(\boldsymbol{x}_k, t_k + \tau) \\ &= \boldsymbol{f}_{k+1} + \frac{\boldsymbol{f}_{k+1}/3 + \boldsymbol{f}_k/2 - \boldsymbol{f}_{k-1} + \boldsymbol{f}_{k-2}/6}{\eta}\tau \\ &+ \frac{\boldsymbol{f}_{k+1}/2 - \boldsymbol{f}_k + \boldsymbol{f}_{k-1}/2}{\eta^2}\tau^2 \\ &+ \frac{\boldsymbol{f}_{k+1}/6 - \boldsymbol{f}_k/2 + \boldsymbol{f}_{k-1}/2 - \boldsymbol{f}_{k-2}/6}{\eta^3}\tau^3 \end{aligned} \tag{20}$$

Comparing Eq.(20) with Eq.(15), the recursion formula is then established as,

$$\boldsymbol{u}_{k+1} = \boldsymbol{\Phi}\boldsymbol{u}_k + \eta(\bar{\boldsymbol{\Phi}}_0\boldsymbol{f}_{k+1} + \bar{\boldsymbol{\Phi}}_1\boldsymbol{f}_k + \bar{\boldsymbol{\Phi}}_2\boldsymbol{f}_{k-1} + \bar{\boldsymbol{\Phi}}_3\boldsymbol{f}_{k-2}) \tag{21}$$

in which

$$\begin{aligned} \bar{\boldsymbol{\Phi}}_0 &= \boldsymbol{\Phi}_1/3 + \boldsymbol{\Phi}_2/2 + \boldsymbol{\Phi}_3/6 \\ \bar{\boldsymbol{\Phi}}_1 &= \boldsymbol{\Phi}_0 + \boldsymbol{\Phi}_1/2 - \boldsymbol{\Phi}_2 - \boldsymbol{\Phi}_3/2 \\ \bar{\boldsymbol{\Phi}}_2 &= -\boldsymbol{\Phi}_1 + \boldsymbol{\Phi}_2/2 + \boldsymbol{\Phi}_3/2 \\ \bar{\boldsymbol{\Phi}}_3 &= \boldsymbol{\Phi}_1/6 - \boldsymbol{\Phi}_3/6 \end{aligned} \tag{22}$$

The external forces are known and linearly distributed during each time increment in structural engineering, such that the external force can be written as a linear function in the time domain $[t_k, t_{k+1}]$ as Eq.(23) with an exact result provided by Duhamel integration.

$$\mathbf{f}(t_k + \tau) = \mathbf{f}_k + \tau(\mathbf{f}_{k+1} - \mathbf{f}_k)/\eta \tag{23}$$

3.3. Estimation with the explicit method

The explicit method with the three-point forward Lagrange interpolation function may result in inaccurate values (Fig. 1(a)) or even opposite trends (Fig. 1(b)) when large time increments are adopted for the estimation of $\boldsymbol{x}_{k+1}$ in the next time increment. As illustrated in Fig. 1, exact values of functions, sin(πt) and sin3(πt) respectively, are given in red stars. The functions of the four-point forward Lagrange interpolation method over the time domain within four-time increments are shown with colored lines. Time is divided into 30 equal time increments within [-0.5, 1] for each function and t_k is adopted as t = 0.5. 'Lagrange1' represents interpolating with points at t_{k-3}, t_{k-2}, t_{k-1} and t_k, which are the dotted point with red stars. Similarly, 'Largrange2' standards for interpolating with every two points, the points at t_{k-6}, t_{k-4}, t_{k-2} and t_k, etc.

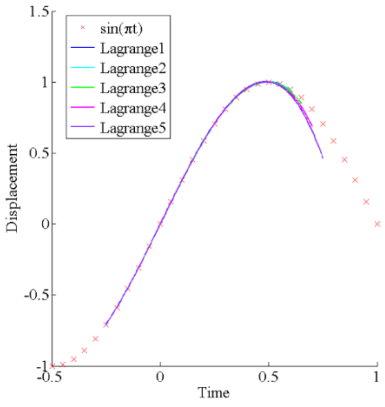

(a) Fitting of sin(πt)

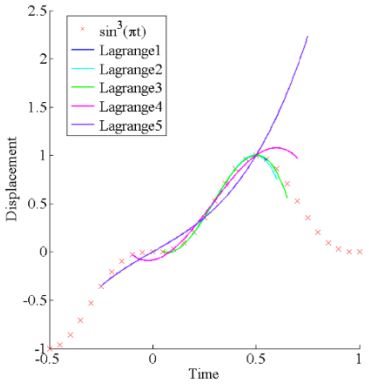

(b) Fitting of sin3(πt)

Fig. 1 Accuracy of the forward Lagrange interpolation with different time increments

As clearly seen in Fig. 1(a), the estimated value for sin(πtk+1) (value for the next time step at time tk+1 for Lagrane1, tk+2 for Lagrane2, etc.) is lower than the exact result, and larger discrepancies are observed in larger time increments even with the right variational trend. Nevertheless, the variational trend of Lagrange interpolation is opposite with large time increments (e.g., Largange4 and Largange5) in Fig. 1(b). The deviation accumulates during the integration with the Duhamel method as well as the recursion formulation in Eq.(13). Thus, estimation with better methods is required to minimize this error.

Totally eight methods with three different orders of accuracy are introduced by adopting the Lagrange interpolation method and the Hermite interpolation method. Due to the ill-condition of high order interpolation function, functions with higher order (e.g., sixth-order and above) are not introduced or considered in this paper.

Third-order $\boldsymbol{O}(\eta^3)$	$\boldsymbol{x}_{k+1,\text{estimate}} = \boldsymbol{x}_{k-1} + 2\eta\boldsymbol{v}_k$	(24)
	$\boldsymbol{x}_{k+1,\text{estimate}} = 3\boldsymbol{x}_k - 3\boldsymbol{x}_{k-1} + \boldsymbol{x}_{k-2}$	(25)
Fourth-order $\boldsymbol{O}(\eta^4)$	$\boldsymbol{x}_{k+1,\text{estimate}} = 2\boldsymbol{x}_k - \boldsymbol{x}_{k-1} + \eta^2\boldsymbol{a}_k$	(26)
	$\boldsymbol{x}_{k+1,\text{estimate}} = 4\boldsymbol{x}_k - 6\boldsymbol{x}_{k-1} + 4\boldsymbol{x}_{k-2} - \boldsymbol{x}_{k-3}$	(27)
	$\boldsymbol{x}_{k+1,\text{estimate}} = -4\boldsymbol{x}_k + 5\boldsymbol{x}_{k-1} + 4\eta\boldsymbol{v}_k + 2\eta\boldsymbol{v}_{k-1}$	(28)
	$\boldsymbol{x}_{k+1,\text{estimate}} = -3\boldsymbol{x}_k/2 + 3\boldsymbol{x}_{k-1} - \boldsymbol{x}_{k-2}/2 + 3\eta\boldsymbol{v}_k$	(29)
Fifth-order $\boldsymbol{O}(\eta^5)$	$\boldsymbol{x}_{k+1,\text{estimate}} = -9\boldsymbol{x}_k + 9\boldsymbol{x}_{k-1} + \boldsymbol{x}_{k-2} + 6\eta\boldsymbol{v}_k + +6\eta\boldsymbol{v}_{k-1}$	(30)
	$\boldsymbol{x}_{k+1,\text{estimate}} = 15\boldsymbol{x}_k/4 - 3\boldsymbol{x}_{k-1} + \boldsymbol{x}_{k-2}/4 - 3\eta\boldsymbol{v}_k/2 + 3\eta^2\boldsymbol{a}_k/2$	(31)

The explicit-implicit method with each estimation function from Eq.(24) to Eq.(31) is defined as EIPIM_O31, EIPIM_O32, EIPIM_O41, EIPIM_O42, EIPIM_O43, EIPIM_O44, EIPIM_O51, and EIPIM_O52, respectively, indicating the order of accuracy. The EIPIMs stand for a total of eight methods with different estimation functions.

4. The algorithm of EIPIM

For nonlinear analysis with stiffness matrix K depending on displacements of structures, the recursion formula of EIPIM is given in Eq.(32) based on the RPIM, before which, the estimation functions in Eq.(24) to Eq.(31) should be employed for $\boldsymbol{x}_{k+1,\text{estimate}}$ and $\mathbf{K}_{k+1,\text{estimate}}$ is evaluated with $\boldsymbol{x}_{k+1,\text{estimate}}$ thereafter. In linear analysis, $\mathbf{K}_{k+1,\text{estimate}}$ should be replaced by constant K.

$$\begin{aligned}\boldsymbol{x}_{k+1} &= \boldsymbol{x}_k + \boldsymbol{T}_{12}\boldsymbol{v}_k + \eta\mathbf{M}^{-1}[\Phi_{01}\boldsymbol{f}_k + \Phi_{11}(\boldsymbol{f}_{k+1} - \boldsymbol{f}_k)] \\ &\quad + \eta\mathbf{M}^{-1}\big(\bar{\Phi}_{01}\mathbf{K}_{k+1,\text{estimate}}\boldsymbol{x}_{k+1,\text{estimate}} \\ &\quad + \bar{\Phi}_{11}\mathbf{K}_k\boldsymbol{x}_k + \bar{\Phi}_{21}\mathbf{K}_{k-1}\boldsymbol{x}_{k-1} \\ &\quad + \bar{\Phi}_{31}\mathbf{K}_{k-2}\boldsymbol{x}_{k-2}\big) \\ \boldsymbol{v}_{k+1} &= \boldsymbol{T}_{22}\boldsymbol{v}_k + \eta\mathbf{M}^{-1}[\Phi_{02}\boldsymbol{f}_k + \Phi_{12}(\boldsymbol{f}_{k+1} - \boldsymbol{f}_k)] \\ &\quad + \eta\mathbf{M}^{-1}\big(\bar{\Phi}_{02}\mathbf{K}_{k+1,\text{estimate}}\boldsymbol{x}_{k+1,\text{estimate}} \\ &\quad + \bar{\Phi}_{12}\mathbf{K}_k\boldsymbol{x}_k + \bar{\Phi}_{22}\mathbf{K}_{k-1}\boldsymbol{x}_{k-1} \\ &\quad + \bar{\Phi}_{32}\mathbf{K}_{k-2}\boldsymbol{x}_{k-2}\big)\end{aligned} \tag{32}$$

The difference of algorithms between the EIPIM and RPIM is that the displacements and stiffness matrix should be estimated before the calculation of displacements and velocities for the next time increment. In this paper, the CDM is adopted to calculate the required results at the first two or three steps for both linear and nonlinear problems, as illustrated in Fig. 2. The first two steps are needed in the EIPIM_O31, EIPIM_O32, EIPIM_O41, and EIPIM_O43 because there is no requirement either on displacement at time tk-1 or velocity at time tk-2. Acceleration should be updated if involved in estimation formulae, such as the EIPIM_O41 and EIPIM_O52.

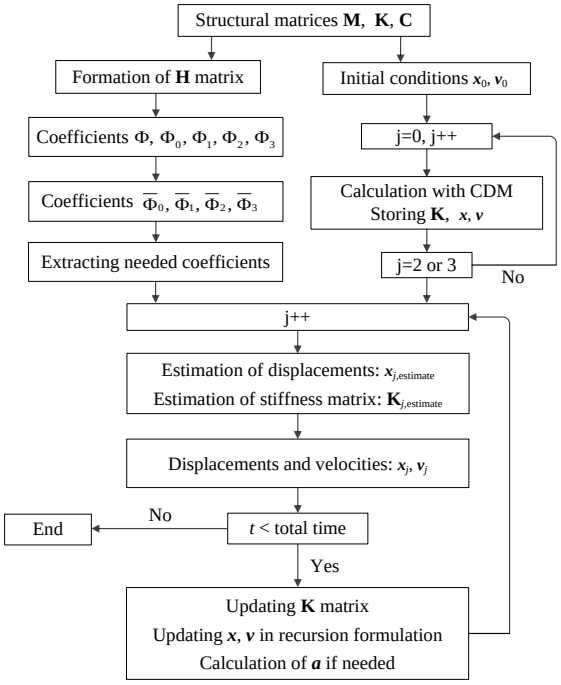

Fig. 2 Algorithm flowchart of EIPIM

5. Stability and precision analysis

In this section, we analyze the two most important characteristics of an algorithm [41], stability and precision, and compare the performance of EIPIM with RPIM.

5.1. Stability analysis

The recursion formula is unconditionally stable if the solution will not magnify without limits at any step time. The authors verified the stability of RPIM, and unconditional spectral stability in theory with the spectral radius of $\boldsymbol{\Phi}$ smaller than 1 in another paper. Nevertheless, the approximation in Duhamel integration over time tk (current time) and tk+1 (time at next step) in Eq.(13) may lead to instability due to the unknown function of internal force, multiplication of stiffness matrix K, and displacements x. In the RPIM, the explicit Lagrange interpolation method with four previous K and x is adopted in recursion formula. As illustrated in Fig. 1, unsuitable functions, with large time increments for the next step, will produce wrong tendencies. The implicit Lagrange interpolation method is employed in the EIPIM in Eq.(20) and better stability will be provided if the estimation of displacement at time tk+1 is accurate enough.

For the eight EIPIMs, estimation formulas with third-order, forth-order and fifth-order accuracy involving displacements, velocities, and accelerations may have different effects on the stability of recursion formula. Among these methods, EIPIM_O32 and EIPIM_O42 only adopting displacements in estimation function, which is the Lagrange interpolation method mathematically, means that only displacements are satisfied at the discretized time points. Methods with velocity and/or acceleration involved in estimation function (Hermit interpolation function, in essence), satisfy not only the displacement but also the velocity/acceleration at certain time points. The EIPIM_O41 achieves the fourth-order accuracy with only three parameters, reducing the accumulation of initial magnitude error—error resulting from inaccurate initial parameters used to make an estimation. Thus, the EIPIM_O41 exhibits the highest stability theoretically. The EIPIM_O51 and EIPIM_O52 may become unstable with relatively smaller time increments due to the ill-condition of interpolation functions with higher order accuracy.

5.2. Precision analysis

For both the EIPIM and RPIM, integration of inhomogeneous terms Kx is the only approximation during the derivation of recursion formula for equation of motion. The RPIM with the fourth order explicit Lagrange interpolation function has a precision of $O(\Delta t^5)$ which is closely related to the time increment Δt.

With a similar derivation process, the recursion formulation of Eq.(8) can be written as,

$$\boldsymbol{u}_{k+1} = \boldsymbol{\Phi}\boldsymbol{u}_k + \eta(\bar{\boldsymbol{\Phi}}_0\mathbf{F}_{k+1} + \bar{\boldsymbol{\Phi}}_1\mathbf{F}_k + \bar{\boldsymbol{\Phi}}_2\mathbf{F}_{k-1} + \bar{\boldsymbol{\Phi}}_3\mathbf{F}_{k-2}) \tag{33}$$

Combining the addition theorem and the coefficients in Eq.(22), and expanding the $\mathbf{F}_{k+1}$, $\mathbf{F}_{k-1}$ and $\mathbf{F}_{k-2}$ at $\mathbf{F}_k$ with Taylor series, then Eq.(33) can be derived as,

$$\begin{aligned}\boldsymbol{u}_{k+1} &= \boldsymbol{\Phi}\boldsymbol{u}_k + \eta\bar{\boldsymbol{\Phi}}_0\big(\boldsymbol{u}_k^{(1)} - \boldsymbol{u}_k\big) \\ &\quad + \sum_{j=0}^{\infty}\left(\frac{(\eta)^j}{j!}\bar{\boldsymbol{\Phi}}_1 + \frac{(-\eta)^j}{j!}\bar{\boldsymbol{\Phi}}_2\right. \\ &\quad \left. + \frac{(-2\eta)^j}{j!}\bar{\boldsymbol{\Phi}}_3\right)\big(\boldsymbol{u}_k^{(j+1)} - \boldsymbol{u}_k^{(j)}\big) \\ &= \boldsymbol{u}_k + \eta\boldsymbol{u}_k^{(1)} + \frac{\eta^2}{2}\boldsymbol{u}_k^{(2)} + \frac{\eta^3}{6}\boldsymbol{u}_k^{(3)} \\ &\quad + \frac{\eta^4}{24}\boldsymbol{u}_k^{(4)} \\ &\quad + \frac{\eta^5}{24}\Big(\frac{5}{6}\boldsymbol{u}_k^{(5)} + \frac{31}{30}\mathbf{H}\boldsymbol{u}_k^{(4)} + O(\eta)\Big) + \cdots\end{aligned} \tag{34}$$

Thus, the EIPIM with implicit Lagrange interpolation function has the precision of $O(\Delta t^5)$, the same accuracy as the RPIM in theory.

6. Verification examples

Several examples are analyzed to assess the stability and efficiency of the proposed EIPIMs in dealing with linear and nonlinear dynamic analysis. The free vibration and forced vibration with constant and varied external forces of a cantilever are studied to provide better understanding and easier duplication of the EIPIMs, as well as a demonstration in a linear analysis. Besides the proposed EIPIMs with eight different estimation functions, results from the other three different methods, namely ODE45(MATLAB), CDM, and RPIM, are given and compared with EIPIMs in linear dynamic analysis. The results from function ode45 [42] in MATLAB are used as references, in which the fourth-order and fifth-order Runge-Kutta algorithm are adopted, commonly used for nonstiff problems. In nonlinear dynamic analysis, results from MATLAB is not available because of its disability in nonlinear analysis.

6.1. Free vibration of a linear elastic cantilever

A linear elastic cantilever with initial displacement as shown in Fig. 3 is employed to verify the accuracy and stability of the EIPIMs. The beam is divided into ten beam-column elements with equal length. Three DOFs are considered for each node, namely axial displacement, vertical displacement, and rotation. The element mass matrix m and element stiffness matrix k are given as follows, with elastic modulus E=2.0×1010N/m2, the length of element l=0.4m (total length of beam L=4m), section area A=0.1m2, second moment of inertia I=1/480m4. The damping matrix is proportional to the mass matrix with the relationship C=0.2M. Elemental matrices are assembled to the global matrix according to DOFs of each node. The cantilever with initial displacements is illustrated in Fig. 3 with dashed lines. The maximum displacement at the free tip is 1m, and the initial displacements vary with the cubic of distances from the clamped edge at each node. The initial velocity is a zero vector, indicating no initial velocity.

$$\mathbf{m} = \frac{\rho A l}{2}\begin{bmatrix} 1 & & & & & & \\ & 1 & & & & & \\ & & 1 & & & & \\ & & & 1 & & & \\ & & & & 1 & & \\ & & & & & 1 & \end{bmatrix}$$

$$\mathbf{k} = \begin{bmatrix} \frac{EA}{l} & 0 & 0 & -\frac{EA}{l} & 0 & 0 \\ & \frac{12EI}{l^3} & \frac{6EI}{l^2} & 0 & -\frac{12EI}{l^3} & \frac{6EI}{l^2} \\ & & \frac{4EI}{l} & 0 & -\frac{6EI}{l^2} & \frac{2EI}{l} \\ & s & & \frac{EA}{l} & 0 & 0 \\ & & m & & \frac{12EI}{l^3} & -\frac{6EI}{l^2} \\ & & & y & & \frac{4EI}{l} \end{bmatrix}$$

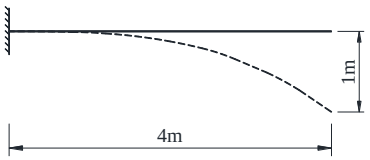

Fig. 3 Configuration of a linear cantilever beam

Typical time-displacement curves with certain time increments are illustrated in Fig. 4. For time increment Δt = 0.00004s, results from EIPIM with the fifth order-accuracy, EIPIM_O51, and EIPIM_O52 exhibit instability as shown in Fig. 4(a), while other methods can still give reasonable predictions of displacements. This is primarily due to the ill-condition of higher order interpolation, as discussed in section 3.3. When time increment increases to Δt = 0.00011s as shown in Fig. 4(b), the RPIM starts to become unstable at the very beginning at about 0.003s, and EIPIM_O32, EIPIM_O42, EIPIM_O51, and EIPIM_O52 all suffer instability in only 0.03s. As shown in Fig. 4(b), results from the CDM vary quite a lot from the exact results of MATLAB, while other methods (EIPIM_O31, EIPIM_O41, EIPIM_O43, and EIPIM_O44) provide estimations much closer to exact solutions.

It should be noted that the results from the EIPIM_O42 are the same as those from the RPIM. This is due to the constant stiffness matrix and the same estimation method, fourth-order Lagrange interpolation method. To be specific, the combination of explicit fourth-order Lagrange interpolation method for estimation and implicit fourth-order Lagrange interpolation method to calculate displacement at the next step in the EIPIM_O42 results in the same function during the time domain, which is also the same as explicit Lagrange interpolation method in the recursion formula of the RPIM. Due to the constant stiffness matrix in linear elastic problems, the same coefficient is multiplied to displacements, and thus EIPIM_O42 and RPIM yield to the same solutions resulting from the same function for displacements, which will also be applicable in section 6.2.

As shown in Fig. 4(c), for the time increment Δt = 0.00016s, only the EIPIM_O31 and EIPIM_O41 can provide reasonable results being close to those from MATLAB. When the time increment increases, the EIPIM can no longer give stable result. Nevertheless, the stable time limit Δt = 0.00016s of the EIPIM_O31 and EIPIM_O41 is more than 1.5 times larger than Δt = 0.0001s of RPIM, indicating superior stability of the EIPIM_O31 and EIPIM_O41.

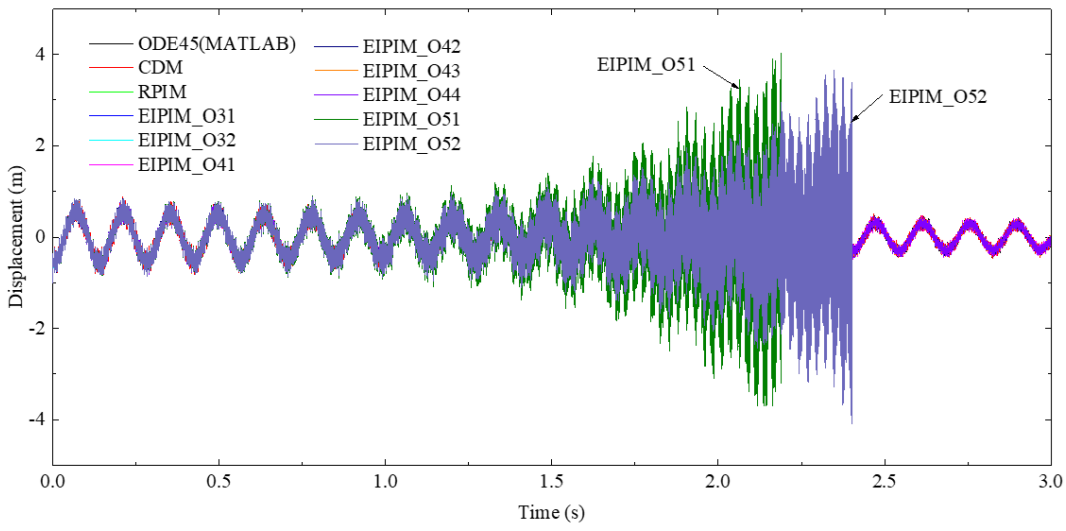

(a) Time-displacement curve with time increment Δt = 0.00004s

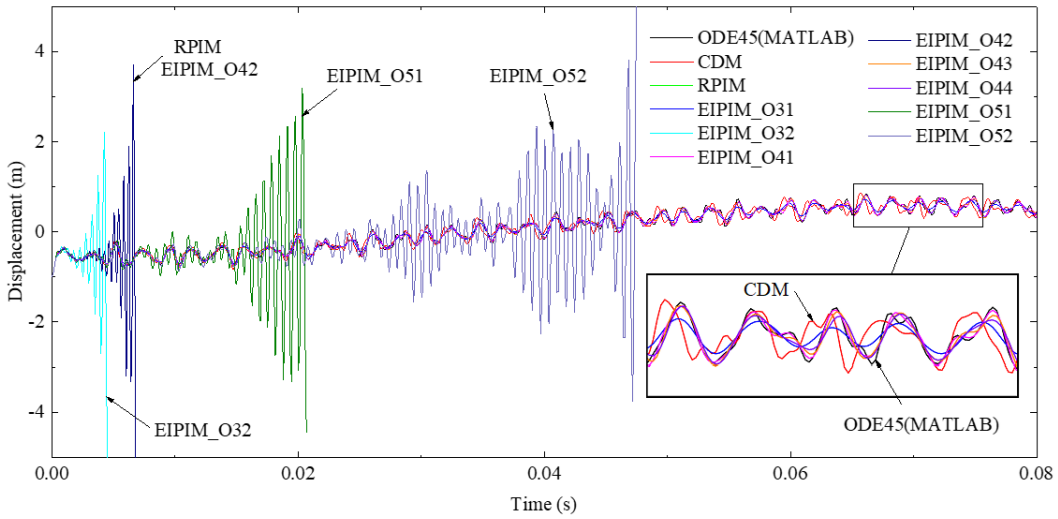

(b) Time-displacement curve with time increment Δt = 0.00011s

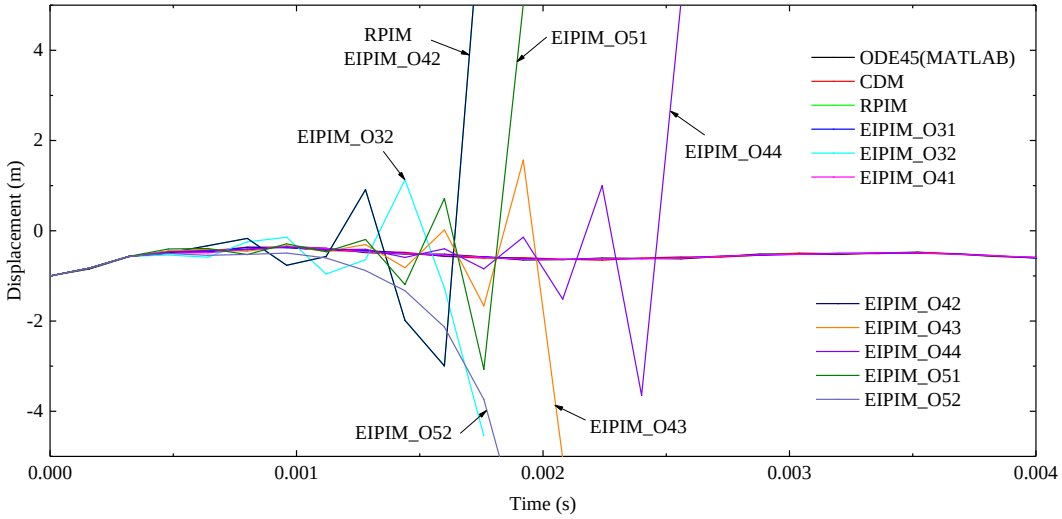

(c) Time-displacement curve with time increment Δt = 0.00016s

Fig. 4 Time-displacement curves of the cantilever beam with free vibration

6.2. Forced vibration of a linear elastic cantilever

In this example, a cantilever beam, with the same section and material properties and the same boundary condition as in section 6.1, is employed. The differences lie in both null vectors of initial displacement and velocity, and the constant vertical external force on free tip F=100kN. Similarly, only the displacements at the free tip are monitored for different time increments as illustrated in Fig. 5.

At time increment Δt =0.00007s, the EIPIMs with fifth order accuracy of estimation, EIPIM_O51, and EIPIM_O52, start to be unstable within 0.5s, while stable and reasonable results are obtained from other methods, as shown in Fig. 5(a). The RPIM cannot work well from Δt =0.00011s and the same results are provided with those from EIPIM_O42, as discussed in section 6.1. The EIPIM_O32, EIPIM_51, and EIPIM_O52 could not remain effective at this time increment, as shown in Fig. 5(b). Similar to free variation case, the RPIM and all EIPIMs, except EIPIM_O31 and EIPIM_O41, yield to instability at Δt = 0.00016s, while EIPIM_O31 and EIPIM_O41 provide accurate results very close to those from MATLAB, as illustrated in Fig. 5(c) and (d). Comparing with the results from different methods in section 6.1 with free vibration, the stability of different methods are nearly the same except for small differences in EIPIM_O44, EIPIM_O51, and EIPIM_O52, which will be further compared and discussed at the end of this section.

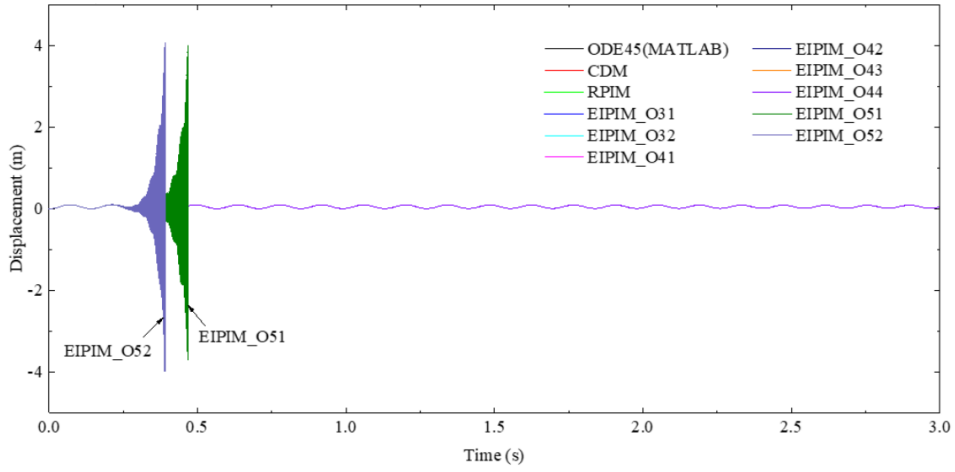

(a) Displacement curve with time increment Δt = 0.00007s

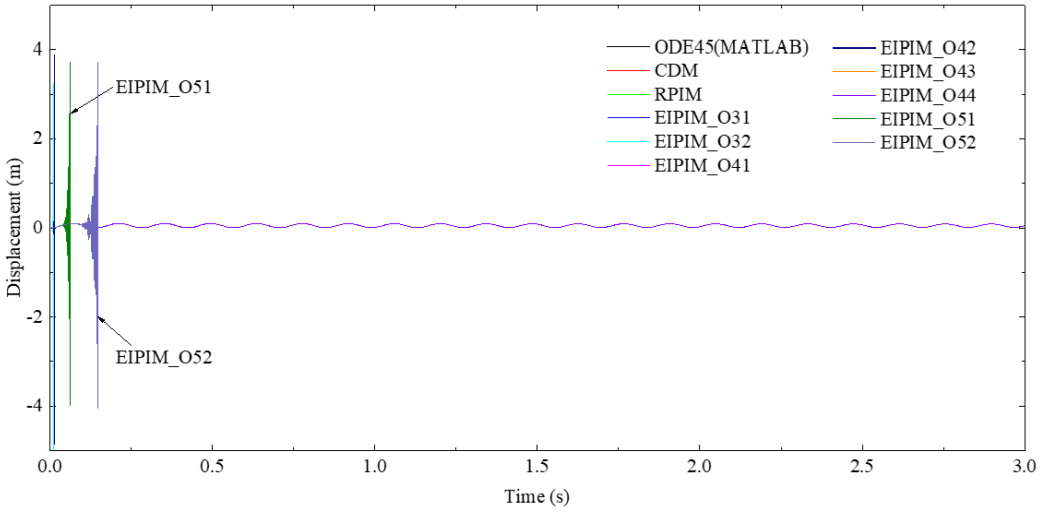

(b1) 0 s ~ 3.0 s

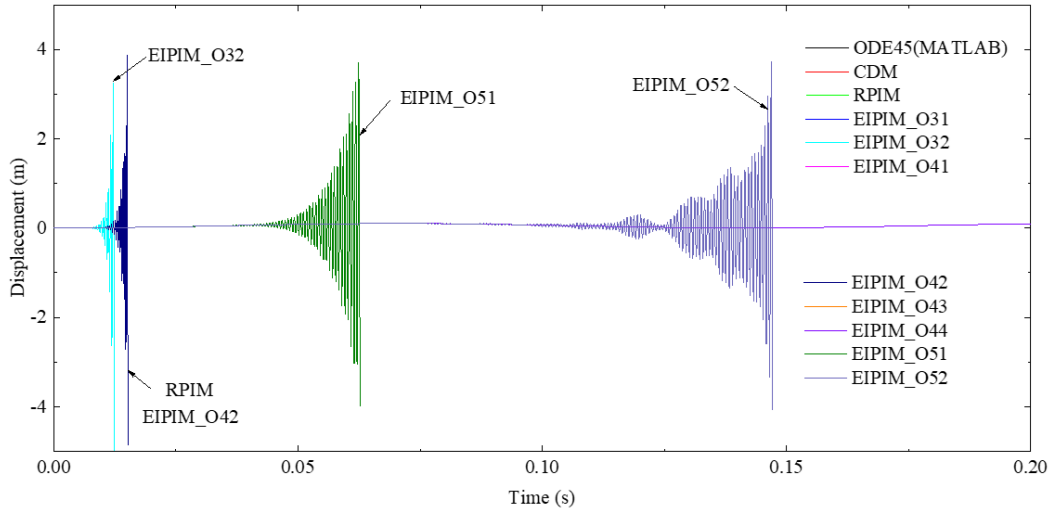

(b2) 0 s ~ 0.2 s

(b) Displacement curve with time increment Δt = 0.00011s

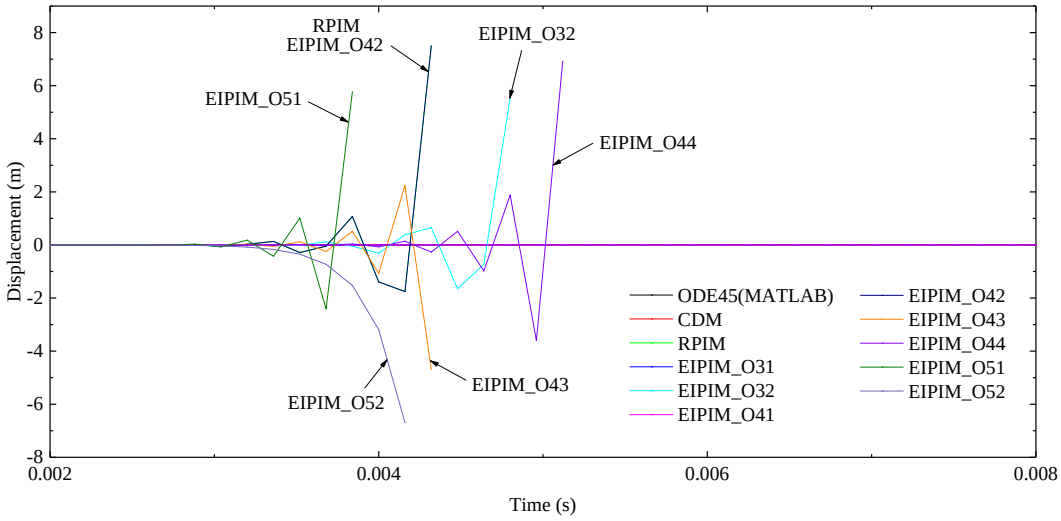

(c) Displacement curve with time increment Δt = 0.00016s

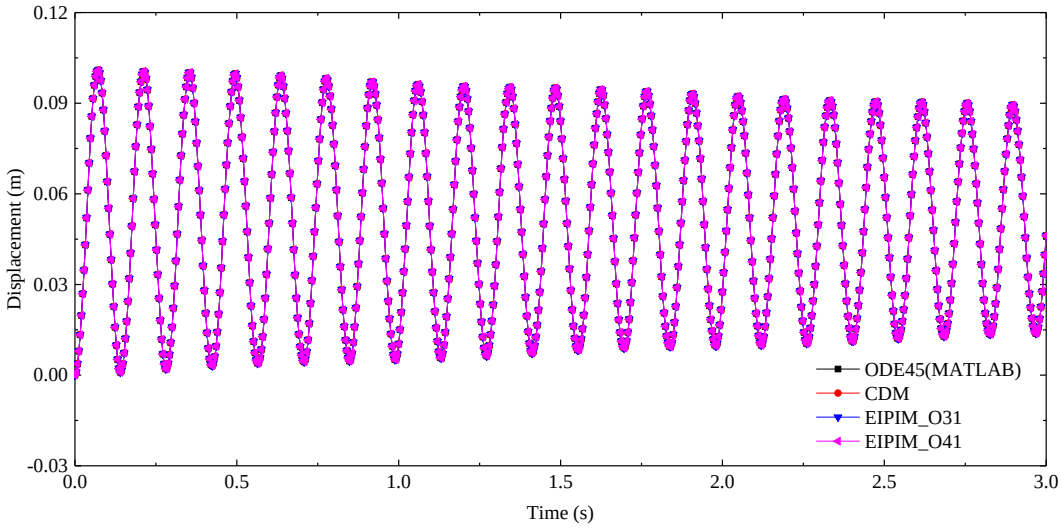

(d) Displacement curves of EIPIM_O31 and EIPIM_O41 with time increment Δt = 0.00016s

Fig. 5 Time-displacement curves of the cantilever with constant force

A varied external force with the same amplitude of load in constant force case multiplying sine function sin(8πt) is adopted in this part to test the stability and accuracy of EIPIMs in regard to a varied external force.

At time increment Δt = 0.00005s, as shown in Fig. 6(a), the EIPIM_O51 and EIPIM_O52 provide a reasonable estimation of displacements at the beginning and start to lose stability at about 1.8s with largely oscillated results from about 2.2s, demonstrating the ill-condition of higher order interpolation method again. The same as in free vibration and vibration with constant force, the RPIM starts to be ineffective from time increment Δt = 0.00011s and yields instability at the very beginning (Fig. 6(b)), while the EIPIM_O31 and EIPIM_O41 still provide accurate results when Δt = 0.00016s (Fig. 6(d)).

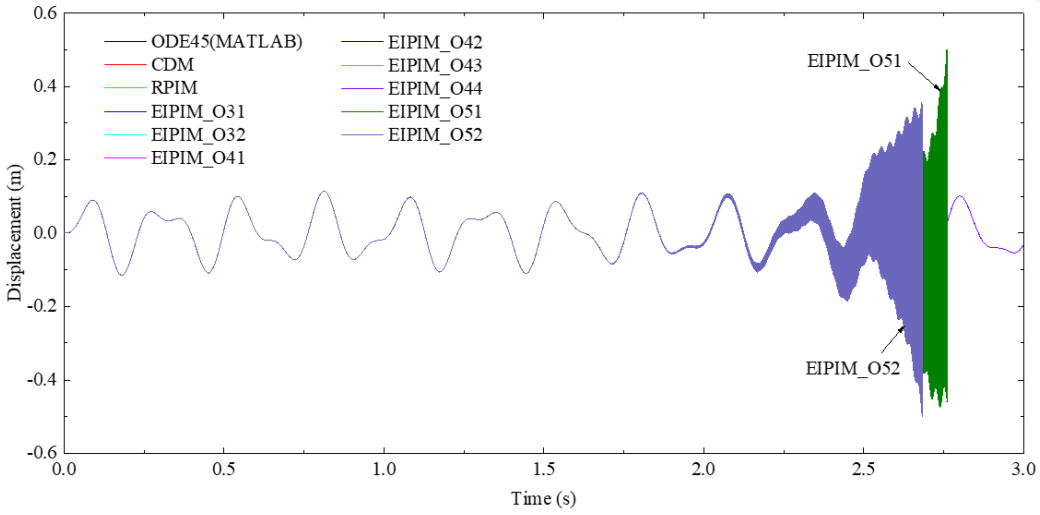

(a) Displacement curve with time increment Δt = 0.00005s

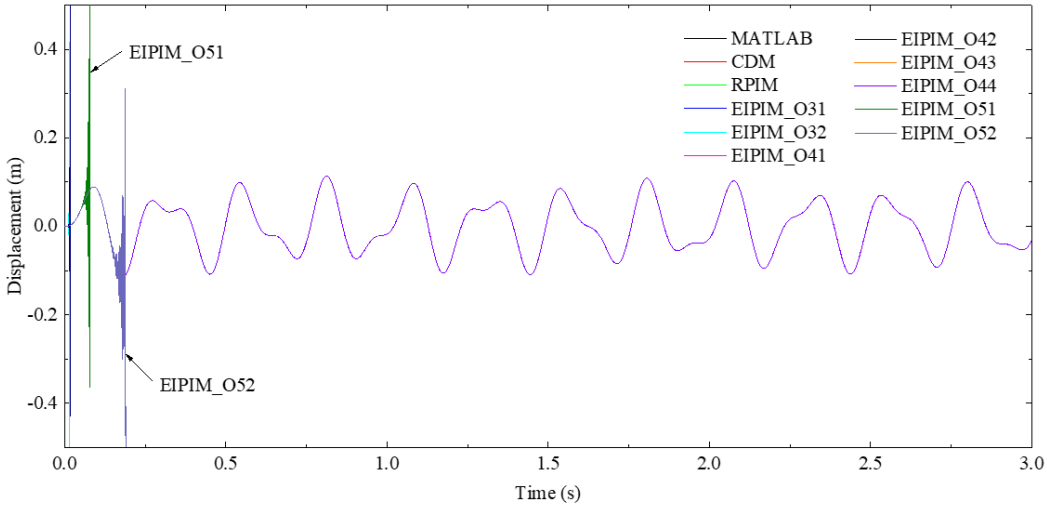

(b1) 0 s ~ 3.0 s

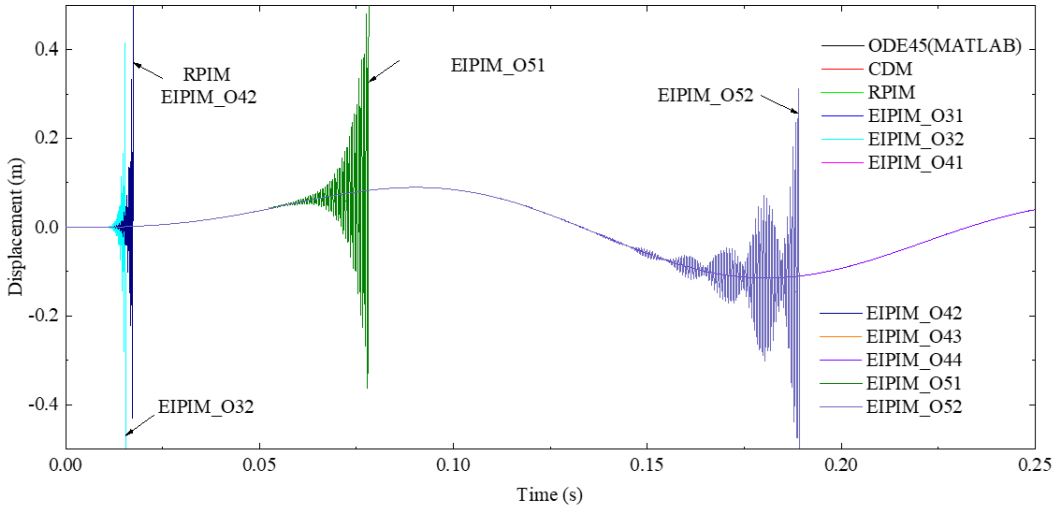

(b2) 0 s ~ 0.25 s

(b) Displacement curve with time increment Δt = 0.00011s

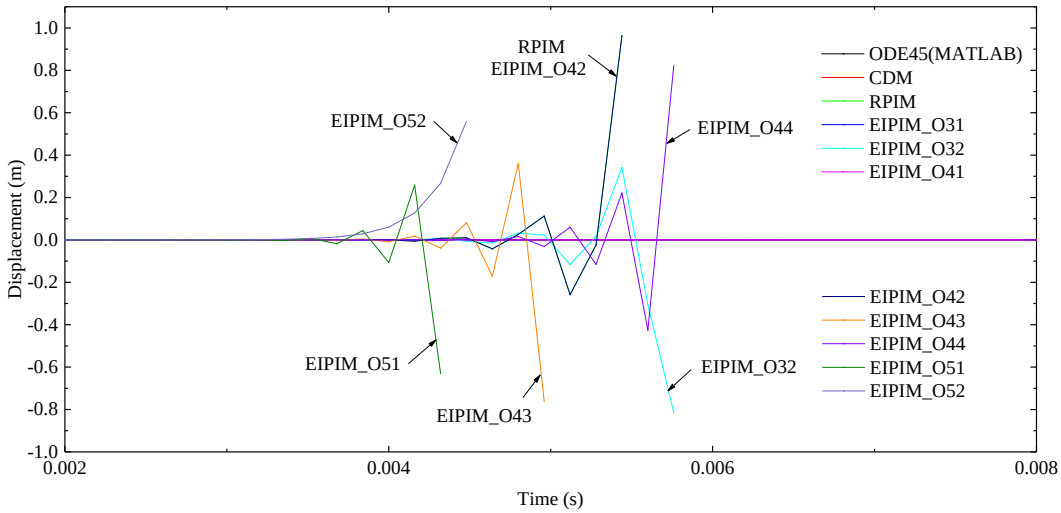

(c) Displacement curve with time increment Δt = 0.00016s

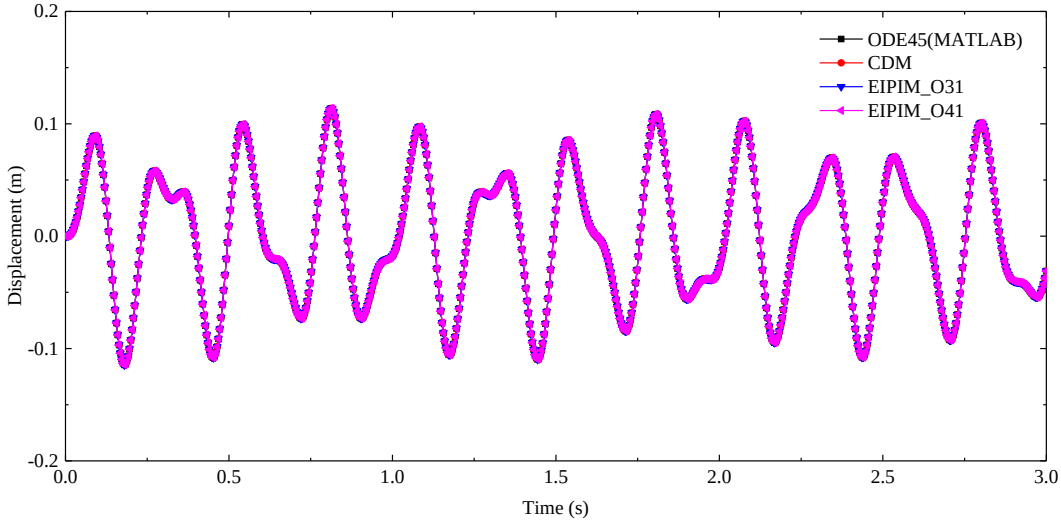

(d) Displacement curves of EIPIM_O31 and EIPIM_O41 with time increment Δt = 0.00016s

Fig. 6 Time-displacement curves of the cantilever with sine force

The stable time limits of different methods in free vibration forced vibration with constant force, and varied force are illustrated in Fig. 7; 'EIPIM_' is omitted for EIPIMs to show the tendency of stability clearly. The same stable time limits are observed for each method, except little differences in EIPIM_O44, EIPIM_O51, and EIPIM_O52, demonstrating the reliability of EIPIMs in dealing with different forms of external loads and initial displacements of the same structure. Among all the EIPIMs, methods with fifth-order accuracy (EIPIM_O51 and EIPIM_O52) exhibit lower stability than the original RPIM, and EIPIM_O32 has a little lower stability than RPIM. EIPIM_O31 and EIPIM_O41 have the highest stability, 60% percent higher

than the RPIM, while the EIPIM_O44 and EIPIM_O43 have relative higher stability. Conclusions could be drawn that estimation function with fifth order accuracy and Lagrange interpolation method (EIPIM_O32 and EIPIM_O42) are not suitable to be incorporated in EIPIM. Higher order interpolation method exhibits certain ill-condition as discussed earlier, and the Lagrange interpolation method only employs the displacements, which lacks the evaluation with velocity and acceleration. In summary, EIPIM_O31 and EIPIM_O41 are recommended for linear dynamic analysis due to their excellent stability.

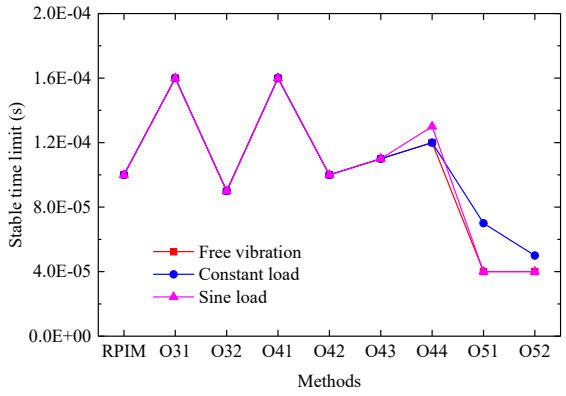

Fig. 7 Stable time limits of different methods for cantilever

The normalized CPU time of the RPIM, EIPIM_O31, and EIPIM_O41 at corresponding stable time limits for free vibration, forced vibration with constant force, and sine force are listed in Table 1.

Table 1
Comparison of CPU time of RPIM, EIPIM_O31, and EIPIM_O32

Methods	Stable time limit (s)	Free vibration	Constant force	Sine force
RPIM	0.0001	1.00	1.00	1.00
EIPIM_O31	0.00016	0.50	0.67	0.68
EIPIM_O41	0.00016	0.65	0.75	0.70

As seen in Table 1, about 60% CPU time is consumed by the EIPIM_O31 and EIPIM_O41 compared with the RPIM for free vibration and about 70% for forced vibration with constant force and sine force. The efficiency of EIPIM_O31 and EIPIM_O41 is superior to the RPIM benefiting from the increased stable time limits. It should also be noted that CPU time of EIPIM_O41 for each case is a little longer than that of EIPIM_O31, and this is because accelerations are required to be calculated in each step while there is no necessity for EIPIM_O31.

6.3. Nonlinear dynamic analysis of truss

In this example, a two-dimensional truss with two DOFs (i.e., horizontal and vertical displacements) for each node [43-44] is shown in Fig. 8. It is modeled by the truss element with geometric nonlinearity considered. The truss is fixed at two ends and external load P=2000kN is applied at nodes 1~7 simultaneously, remaining constant during the analysis. The section and material information are listed as, section area A=0.01m2, elastic modulus E=2.06×1011N/m2, density ρ=7870kg/m3. Its layout and load pattern are illustrated in Fig. 8.

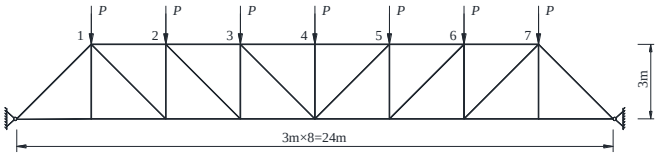

Fig. 8 Loading and boundary conditions of truss

The displacement at node 4 is monitored and the curves at different time increments are shown in Fig. 9. At time increment Δt = 0.00025s (Fig. 9(a)), the EIPIM_O51 and EIPIM_O52 cannot remain stable, while all other methods provide satisfying results. When time increment increases to 0.00045s (Fig. 9(b)), the RPIM can no longer remain stable and yields oscillation from about 0.06s. At this time increment, EIPIM_O32 and EIPIM_O42, the two methods with Lagrange interpolation, are unstable as well. It is noteworthy that results provided by the RPIM and EIPIM_O42 vary, differing from the same results by RPIM and EIPIM_O42 in cases with linear elastic problems (section 6.1 and 6.2), resulting from the changing stiffness matrix during the nonlinear dynamic analysis. Nevertheless, not many differences are observed with regard to the starting time of instability or the tendency of discrepancy. The EIPIM_O31 and EIPIM_O41 are able to give reasonable results with satisfying accuracy at time increment Δt = 0.00065s (Fig. 9(d)), 62.5% higher than the stable time Δt = 0.0012s of RPIM., when other methods all lose effectiveness (Fig. 9(c)).

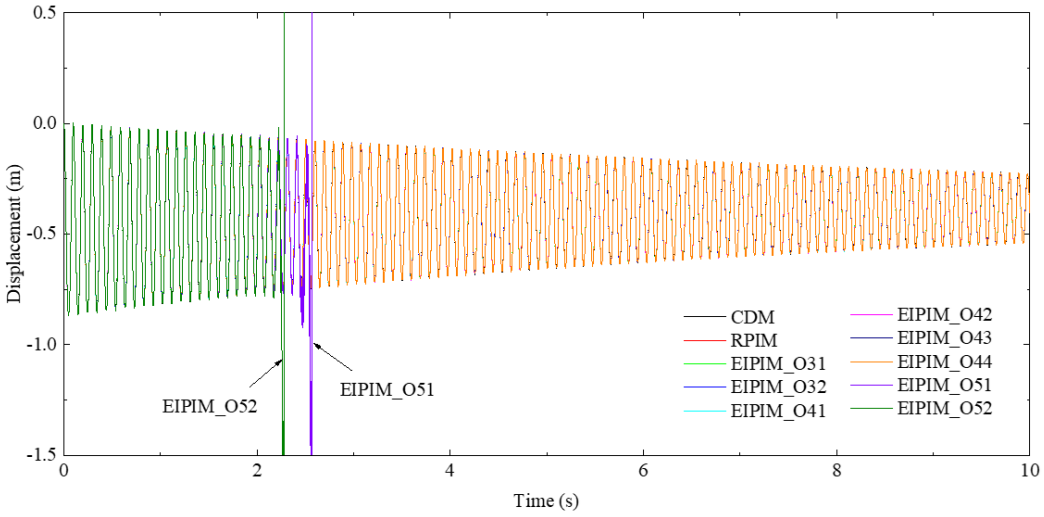

(a) Displacement curve with time increment Δt = 0.00025s

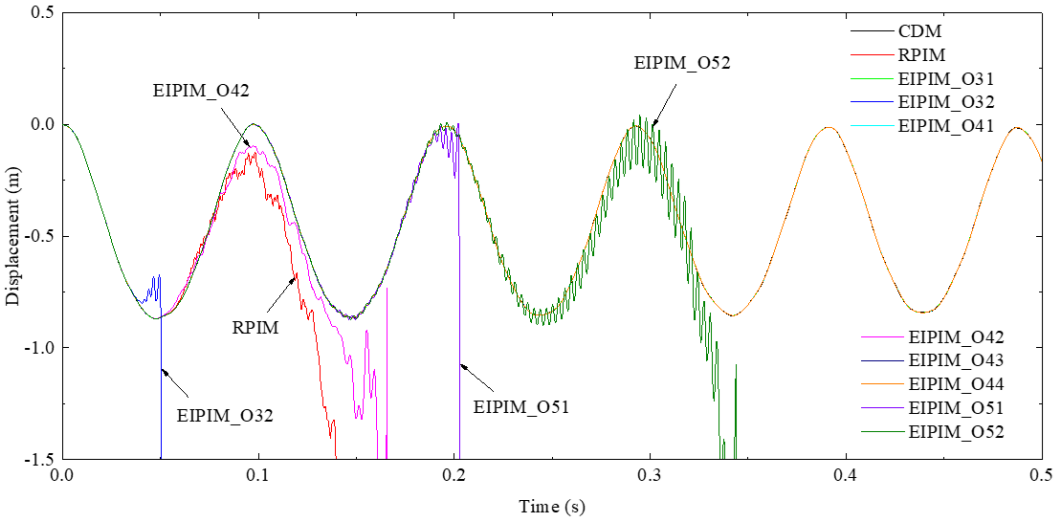

(b) Displacement curve with time increment Δt = 0.00045s

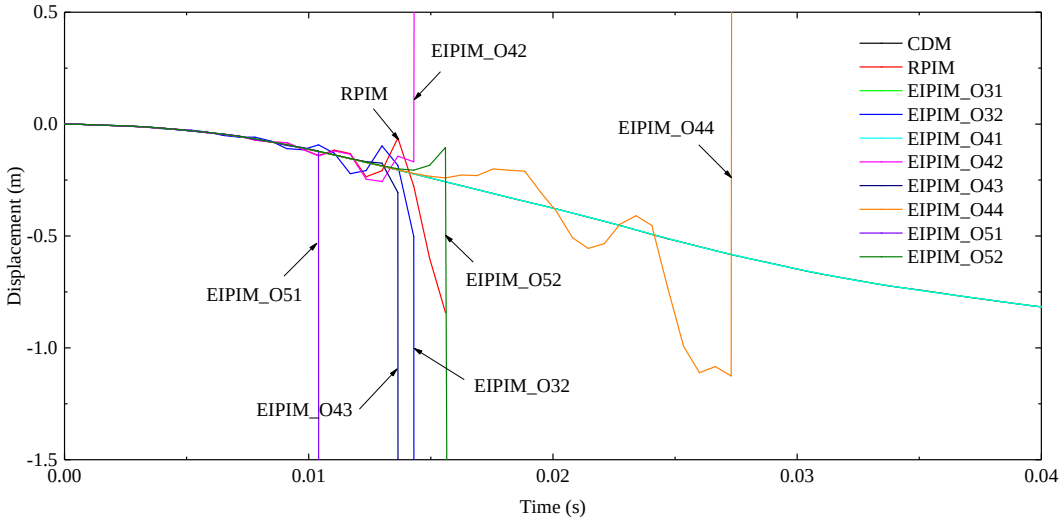

(c) Displacement curve with time increment Δt = 0.00065s

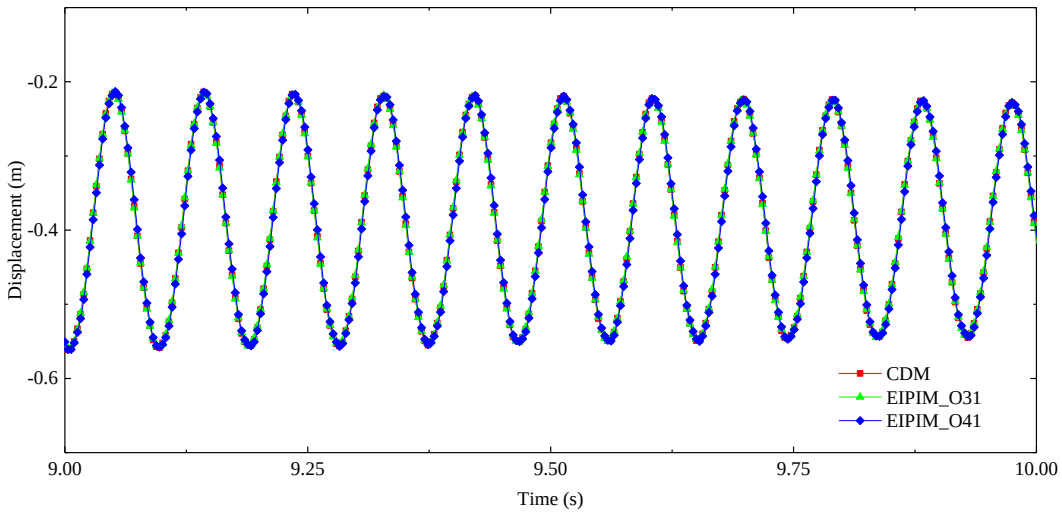

(d) Displacement curves of EIPIM_O31 and EIPIM_O41 with time increment Δt = 0.00065s

Fig. 9 Time-displacement curves of truss with different methods

Stable time limits of each method for the nonlinear truss are illustrated in Fig. 10, and the 'EIPIM_' is also omitted as in Fig. 7 for simplicity. As can be seen, methods with fifth order accuracy exhibit lower stable time limits than the RPIM, while the stability of EIPIM_O32 and EIPIM_O42 with Lagrange interpolation method is close to that of RPIM. Similar to the linear elastic problem, EIPIM_O31 and EIPIM_O41 exhibit the most excellent stability with stable time limit 0.00065s. EIPIM_O43 and EIPIM_O44 possess the same stable time limit 0.00045s, a little higher than that of RPIM. In this case, EIPIM_O31 and EIPIM_O41 are the most suitable methods for nonlinear dynamic analysis of trusses.

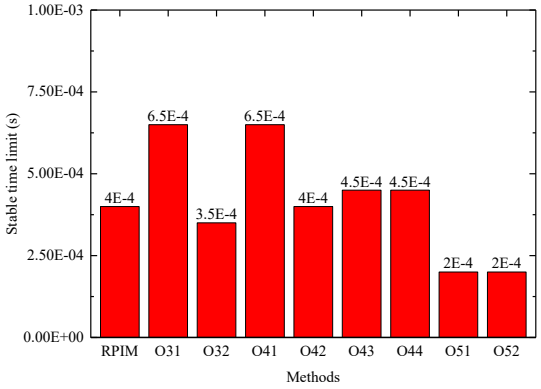

Fig. 10 Stable time limits of different methods for nonlinear truss

Differing from linear cases, CPU time of EIPIM_O31 and EIPIM_O41 at stable time limit 0.0065s is about 85% and 90% respectively of that consumed by the RPIM at stable time limit 0.0004s. Additional estimation of the stiffness matrix is involved in nonlinear cases compared with linear cases, which is time-consuming. Nevertheless, the increased computational effort is compensated by a larger stable time limit, demonstrating the efficiency of EIPIM_O31 and EIPIM_O41 for nonlinear analysis.

6.4. Nonlinear analysis of Mindlin plate

In this verification example, the shell element based on Mindlin plate theory [43] with geometric nonlinearity is employed to model a plate as shown in Fig. 11. The four-node shell element with two-point Gauss integration for bending and one-point Gauss integration for shear is adopted with the shear correction factor 5/6. For each node, there are five DOFs, two in-plane translation, one out-plane translation and two rotations [44]. In Fig. 11, a 2m×2m square plate with ten by ten mesh configuration is employed, with consistent thickness t=0.1m. It is subjected to uniform pressure P=100kN/m2, remaining constant during the nonlinear dynamic analysis. Simple boundary condition with constrained translations and free rotations is employed at nodes along the four external sides. Elastic material with E=2.06×108N/m2, Poisson's ratio ν=0.3, and density ρ=7870kg/m3 is assumed.

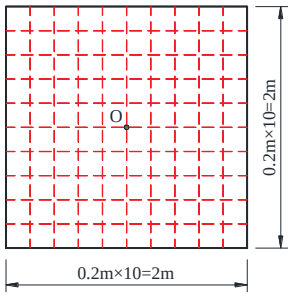

Fig. 11 Configuration of plate

The displacements of the center point O is monitored at different time increments to obtain the stable step limit of each method. Time-displacement curves at selected time increments are illustrated in Fig. 12. From this figure, EIPIM_O51 and EIPIM_O52 suffer instability at a small time increment Δt = 0.0003s, whereas other methods including RPIM are effective with enough accuracy (Fig. 12(a)). Nevertheless, RPIM is not able to provide stable results when time increment is raised to 0.00055s, as well as EIPIM_O32 and EIPIM_O42, the two methods with Lagrange interpolation estimation (Fig. 12(b)). When time increment augments 0.0008s, reasonable results are still available from EIPIM_O31 and EIPIM_O41, as shown in Fig. 12(d), while all the other methods yield to instability, as shown in Fig. 12(c). Conclusions can be drawn that EIPIM_O31 and EIPIM_O41 are the two methods with better stability and accuracy, while EIPIMs with the fifth-order accuracy estimation (EIPIM_O51 and EIPIM_O52) are unsuitable for nonlinear dynamic problems of plates.

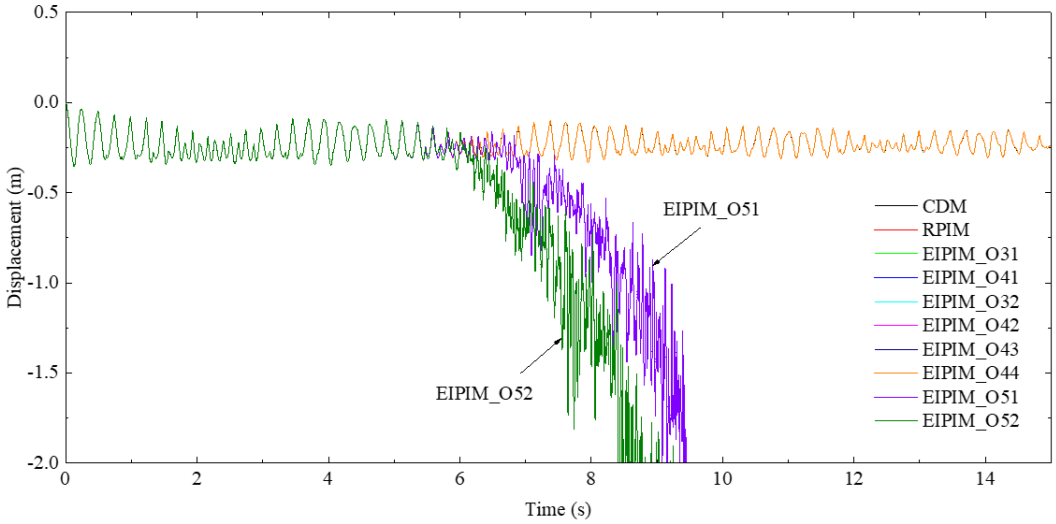

(a) Displacement curve with time increment Δt = 0.0003s

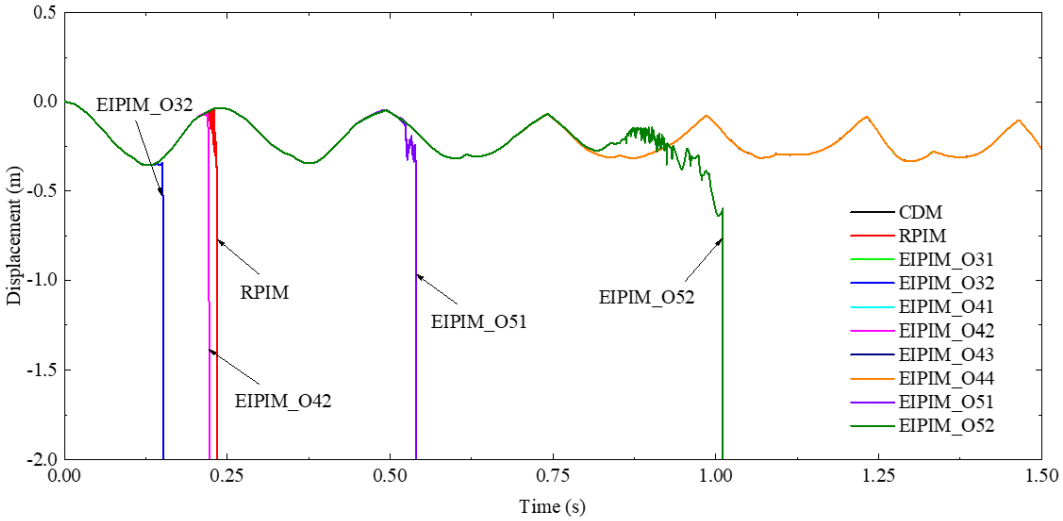

(b) Displacement curve with time increment Δt = 0.00055s

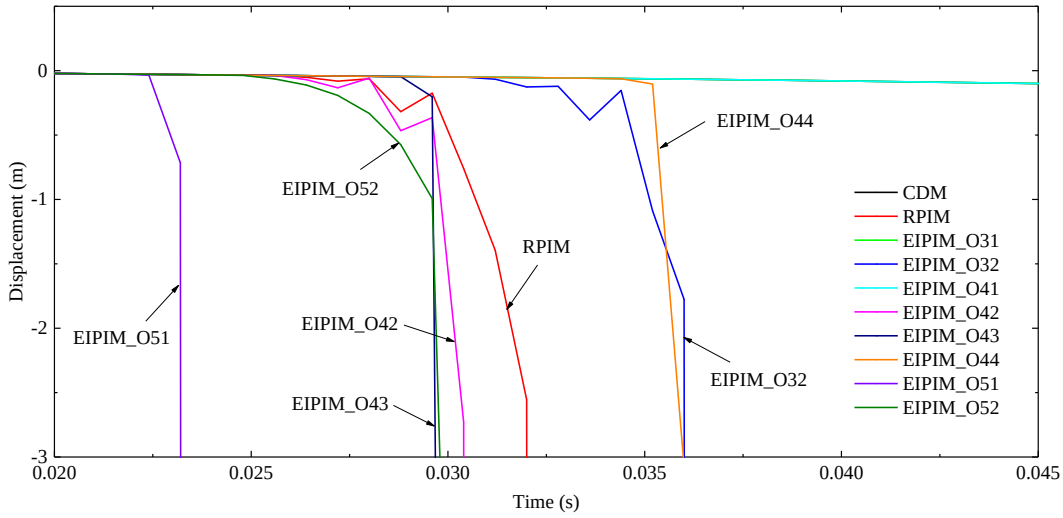

(c) Displacement curve with time increment Δt = 0.0008s

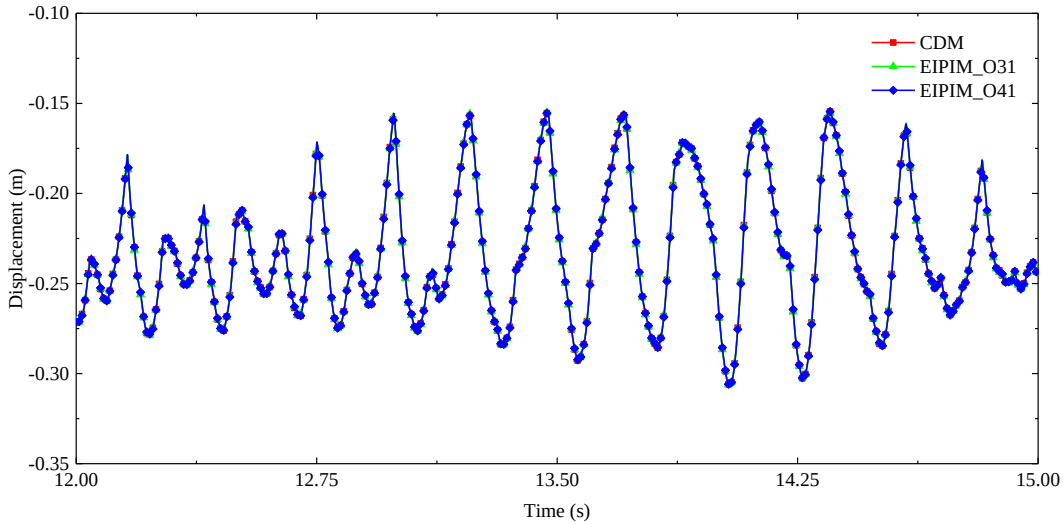

(d) Displacement curves of EIPIM_O31 and EIPIM_O41 with time increment Δt = 0.0008s

Fig. 12 Time-displacement curves of the plate with different methods

To obtain an accurate stable time limit for each method, the time increments are enlarged gradually for all methods with the sub-increment 0.00005s. The stable time limits for each method are figured with 'EIPIM_' omitted as in earlier cases, as shown in Fig. 13. Similar to linear cantilever and nonlinear truss, EIPIM_O51 and EIPIM_O52 have the smallest stable time limit, followed by RPIM, EIPIM_O32, and EIPIM_O42. The EIPIM_O43 and EIPIM_O44 have about 20% higher stable time increment than the RPIM. Meanwhile, EIPIM_O31 and EIPIM_O41 possess the highest stable time limit, 60% higher than that of RPIM, indicating their applicability in nonlinear dynamic analysis of structures.

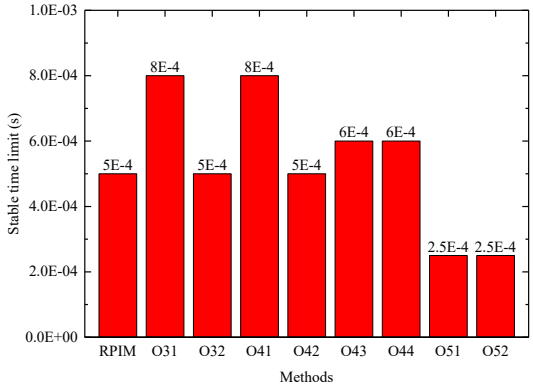

Fig. 13 Stable time limits of different methods for nonlinear plate

It is noteworthy that CPU time of EIPIM_O31 and EIPIM_O41 at the stable time limit is about 80% of that consumed by RPIM at stable time limit 0.0004s, lower than that in the case with nonlinear truss. More computational time could be saved with special procedures to calculate the stiffness matrix since the estimation of the stiffness matrix is the additional part in EIPIMs compared with RPIM. High efficiency of EIPIM_O31 and EIPIM_O41 is achieved with a larger stable time limit for nonlinear analysis, in despite of more computationally demanding in each step.

7. Conclusions

The refined precise integration method (RPIM) has been used for nonlinear dynamic analysis, but it has potential risk due to the numerical instability problem when using large time steps. In this paper, an improved method named the explicit-implicit precise integration method (EIPIM) is proposed based on the conventional RPIM. Eight explicit formulas including second-order, third-order and fifth-order functions have been studied in the framework of the new method. In general, EIPIM has the advantage of better numerical stability and higher precision than the traditional RPIM, and therefore, it has wider applications than RPIM in practical use. Several typical examples demonstrate the numerical stability and computational efficiency of the proposed EIPIM in both linear and nonlinear dynamic analysis.

Several conclusions can be drawn from this study as follows.

(1) EIPIM with higher order interpolation functions does not always perform as well as the lower order ones. For example, the fifth-order EIPIM_O51 and EPIM_O52 exhibit worse stability than RPIM due to the ill-condition of high order interpolation functions.

(2) EIPIMs with Lagrange interpolation functions such as EIPIM_O32 and EIPIM_O42 are not better than RPIM in terms of numerical stability and result precision because only displacements are adopted for the estimation in the next step. EIPIM_O42 provides the same results as RPIM for linear dynamic problems because they are essentially the same, while the different results are obtained from nonlinear dynamic cases due to the variable stiffness matrix.

(3) When fourth-order functions are adopted in the EIPIM, such as EIPIM_O43 and EIPIM_O44, EIPIMs show better performance than RPIM because of the improved accuracy of displacements adopted for the next step.

(4) EIPIM_O31 and EIPIM_O41 exhibit excellent numerical stability in solving both linear and nonlinear dynamic problems; with the time step about 60% larger than RPIM. Thus, the two methods allowing for large time steps are recommended for dynamic analysis of structures.

(5) Generally, EIPIM with Hermit interpolation functions (i.e. EIPIM_O31, EIPIM_O41, EIPIM_O43 and EIPIM_O44) is better than RPIM because the velocities and accelerations (if any) also follow the interpolation procedure used in displacements at each time step, except EIPIM with fifth-order functions due to the ill-condition of higher order interpolation method. The following is an example of two consecutive single-line equations written according to the specifications:

Acknowledgments

The authors are grateful for financial support from "Science and Technology Planning Project of Guangdong Province (2016A050502022) " and the Research Grant Council of the Hong Kong SAR Government on the project "Joint-based second order direct analysis for domed structures allowing for finite joint stiffness (PolyU 152039/18E)".

References

[1] He, Y.J., Zhou, X.H. and Wang, H.S., “Wind-induced response analysis of the cylindrical reticulated mega-structures”, Advanced Steel Construction, 12, 66-82, 2016.
[2] Li Z, Ren H, Tong X, and Li H. , “A Precise Computation Method of Transient Free Surface Green Function”, Ocean Engineering, 105, 318-326,2015.
[3] Zhong W.X., “On precise time integration method for structural dynamics”, Journal of Dalian University of Technology, 34, 131-136, 1994.
[4] Zhong W.X. and Williams F.W., “A precise time step integration method”, Proceedings of the Institution of Mechanical Engineers, Part C: Journal of Mechanical Engineering Science 208, 427-430, 1994.
[5] Gao Q., Tan S.J. and Zhong W.X., “A survey of the precise integration method”, Scientia Sinica Technologica, 46, 1207-1218, 2016.
[6] Wu F., Gao Q. and Zhong W.X., “Subdomain Precise Integration Method for Periodic Structures”, Shock and Vibration, 2014.
[7] Shen W.P., Lin J.H. and Williams F.W., “Parallel computing for the high precision direct integration method”, Computer Methods in Applied Mechanics and Engineering, 126, 315-331, 1995.
[8] Gao Q., Wu F., Zhang H.W., Zhong W.X., Howson W.P. and Williams F.W., “A fast precise integration method for structural dynamics problems”, Structural Engineering and Mechanics, 43, 1-13, 2012.
[9] Lin J.H., Shen W.P. and Williams F.W., “A high precision direct integration scheme for sturctures subjected to transient dynamic loading”, Computers and Structures , 56, 113-120, 1995.
[10] Wang M.F. and Au F.T.K., “Assessment and improvement of precise time step integration method”, Computers and Structures, 84, 779-786, 2006.
[11] Wang M.F. and Au F.T.K., “Precise integration methods based on Lagrange piecewise interpolation polynomials”, International Journal for Numerical Methods in Engineering, 77, 998-1014, 2009.
[12] Zhang,H.W., Zhang X.W. and Chen J.S., “A new algorithm for numerical solution of dynamic elastic-plastic hardening and softening problems” Computers and Structures, 81, 1739-1749, 2003.
[13] Ding Z.X., Du Z.L., Liu Y.P. and Chan S.L., “A refined precise integration method for nonlinear dynamic analysis of structures”, Advanced Steel Construction, 16, 124-136, 2020.
[14] Zhong W.X., “On precise integration method”, Journal of Computational and Applied Mathematics, 163, 59-78, 2004.
[15] Gao Q., Wu F., Zhang H.W., Lin J.H. and Zhong W.X., “A fast precise integration method for large-scale dynamic structures”, Chinese Journal of Computational Mechanics, 28, 492-498, 2011.
[16] Bathe K.J. and Baig M.M.I., “On a composite implicit time integration procedure for nonlinear dynamics”, Computers and Structures, 83, 2513-2524, 2005.
[17] Abaqus 6.17 Documentation. DS SIMULIA Corp, 2017.
[18] The Open System for Earthquake Engineering Simulation. Univeristy of California, Berkeley, 2000.
[19] Newmark N. M., “A Method of Computation for Structural Dynamics,” ASCE, 127, 1406-1432, 1962.
[20] Wilson E.L., Farhoomand I. and Bathe K.J., “Nonlinear dynamic analysis of complex structures”, Earthquake Engineering Structural Dynamics, 3, 241-252, 1972.
[21] Wilson E.L., A Computer Program for the Dynamic Stress Analysis of Underground Structure, 1968.
[22] Mohammad R.P. and Mahdi K.R., “A New Explicit Time Integration Scheme for Nonlinear Dynamic Analysis,” International Journal of Structural Stability and Dynamics, 16, 1550054, 2015.
[23] Du X.Q., Yang D.X., Zhou J.L, Yan X.L., Zhao Y.L. and Li S., “New Explicit Integration Algorithms with Controllable Numerical Dissipation for Structural Dynamics”, International Journal of Structural Stability and Dynamics, 18, 1850044, 2018.
[24] Bathe K.J., “Conserving energy and momentum in nonlinear dynamics : A simple implicit time integration scheme”, Computures and Structures, 85, 437-445, 2007.
[25] Bathe K.J. and Noh G., “Insight into an implicit time integration scheme for structural dynamics”, Computures and Structures, 98, 1-6, 2012.
[26] Noh G. and Bathe K.J., “Further insights into an implicit time integration scheme for structural dynamics”, Computures and Structures, 202, 15-24, 2018.
[27] Zhang J., Liu Y.H. and Liu D.H., “Accuracy of a composite implicit time integration scheme for structural dynamics”, International Journal for Numerical Methods in Engineering, 109, 368-406, 2017.
[28] Kim W. and Choi S.Y., “An improved implicit time integration algorithm: The generalized composite time integration algorithm”, Computures and Structures, 196, 341-354, 2018.
[29] Zienkiewicz O.C. and Xie Y.M., “A simple error estimator and adaptive time stepping procedure for dynamic analysis”, Earthquake Engineering and Structural Dynamics, 20, 871-887, 1991.
[30] Ascher U.M., Ruuth S.J. and Spiteri R.J., “Implicit-explicit Runge-Kutta methods for time-dependent partial differential equations”, Applied Numerical Mathematics, 25, 151-167, 1997.
[31] Lai T, Yi T.H., Li H.N. and Fu X., “An Explicit Fourth-Order Runge-Kutta Method for Dynamic Force Identification”, International Journal of Structural Stability and Dynamics, 17, 1750120, 2017.
[32] Hulbert G.M. and Jang I., “Automatic time step control algorithms for structural dynamics”, Computer Methods in Applied Mechanics and Engineering, 50, 155-178, 1995.
[33] Deokar R., Maxam D. and Tamma K.K., “A novel and simple a posteriori error estimator for LMS methods under the umbrella of GSSSS framework: Adaptive time stepping in second-order dynamical systems”, Computer Methods in Applied Mechanics and Engineering, 334, 414-439, 2018.
[34] Wang L. and Zhong H.Z, “A time finite element method for structural dynamics”, Applied Mathematical Modelling, 41, 445-461, 2017.
[35] Mayr M., Wall W.A. and Gee M.W., “Adaptive time stepping for fluid-structure interaction solvers”, Finite Elements in Analysis and Design, 141, 55-69, 2018.
[36] Rossi D.F., Ferreira W.G., Mansur W.J. andCalenzani A.F.G., “A review of automatic time-stepping strategies on numerical time integration for structural dynamics analysis”, Engineering Structures, 80, 118-136, 2014.
[37] Kuo S.R., Yau J.D. and Yang Y.B., “A robust time-integration algorithm for solving

nonlinear dynamic problems with large rotations and displacements", International Journal of Structural Stability and Dynamics, 12, 1250051, 2012.
[38] Liu Y. and Shen W.P., "Adaptive algotithm of transition matrix in precise integration method", Journal of Vibration and Shock, 2, 82, 1995.
[39] Tan S.J., Gao Q. and Zhong W.X., "Applications of Duhamel term's precise integration method in solving nonlinear differential equations", Chinese Journal of Computational Mechanics, 25, 752-758, 2010.
[40] Alipour A. and Zareian F., "Study Rayleigh Damping in Structures; Unceratinties and Treatments", The 14th World Conference on Earthquake Engineering, Beijing, China, 2008.
[41] Bathe K.J. and Wilson E.L., "Stability and accuracy analysis of direct integration methods", Earthquake Engineering and Structural Dynamics,1, 3-6, 1983.
[42] MATLAB Documentation, MathWorks, 2000.
[43] Bathe K.J., Finite element procedures in engineering analysis, Prentice-Hall, Inc, New Jersey, 1982.
[44] Ferreira A.J.M., MATLAB codes for finite element analysis: solids and structures, Springer, 2008.